Magnetization of multiple-quanta vortex lattices

V. V. Moshchalkov, M. Baert, V. V. Metlushko, E. Rosseel, M. J. Van Bael, and K. Temst
Laboratorium voor Vaste-Stoffysica en Magnetisme, Katholieke Universiteit Leuven, B-3001 Leuven, Belgium

R. Jonckheere
Interuniversity Micro-Electronics Center, Kapeldreef 75, B-3001 Leuven, Belgium

Y. Bruynseraede
Laboratorium voor Vaste-Stoffysica en Magnetisme, Katholieke Universiteit Leuven, B-3001 Leuven, Belgium
(Received 1 December 1995; revised manuscript received 23 May 1996)

We have studied sharp cusplike magnetization (M) anomalies, appearing at matching fields $H_m = m\phi_0/S$ in superconducting films with sufficiently large antidots, forming a regular lattice with a unit-cell area S. Exactly at $H = H_m$ each antidot pins the same quantized flux $m\phi_0$. This $m\phi_0$-flux-line lattice has magnetization $M(H_m) \propto -m\phi_0/\Lambda^2$, where Λ is the penetration depth in the film. Between the matching fields $H_m < H < H_{m+1}$ the $M(H)$ curve follows a simple $M \infty -\ln(H - H_m)$ dependence. As a result, the whole magnetization curve $M(H)$ can now be successfully described by the simple expression, derived for interacting multiquanta vortices in the London limit. In higher fields $H > H_{n_s}$, when the occupancy of the antidots reaches the saturation number $n_s = r/2\xi(T)$, determined by the antidot radius r and temperature-dependent coherence length $\xi(T)$, the ϕ_0 vortices begin to fill interstices, thus forming composite flux-line lattices with $m\phi_0$ vortices strongly pinned by antidots and ϕ_0 vortices weakly pinned by interstices. [S0163-1829(96)07334-1]

I. INTRODUCTION

In 1957 in his classical paper[1] Abrikosov had predicted the existence of the quantum state in homogeneous type-II superconductors. This so-called mixed state is characterized by the formation of the lattice consisting of the flux lines (FL) each carrying *one flux quantum* ϕ_0. To make the penetration of these quantized FL possible, normal vortex cores, with the size given by the temperature-dependent coherence length $\xi(T)$, must be created. Later on, the existence of single-ϕ_0 FL lattices in type-II superconductors without artificially introduced pinning centers has been convincingly demonstrated in magnetic decoration,[2] neutron scattering,[3] and, recently, in scanning tunneling microscope,[4] experiments.

In homogeneous superconductors the formation of the FL lattices consisting of *multiquanta* vortices is energetically unfavorable.[5] Contrary to this, *relatively large artificial pinning centers can stabilize multiquanta vortices*. The maximum possible number of the FL trapped by the single insulating inclusion with the radius r is determined by the saturation number $n_s \cong r/[2\xi(T)]$.[6] For regular arrays of artificial pinning centers the vortex-vortex interactions make the situation more complicated, but still multiquanta FL lattices can exist, provided that the radius r is sufficiently large.[7]

Following the pioneering work of Hebard, Fiory, and Somekh,[8] we have shown recently[9–11] that the *regular arrays of submicron holes* (Fig. 1) (''antidots,'' this definition has been borrowed from the publications[12] on similar nanostructured semiconducting films) can be successfully used to stabilize *multiquanta and interstitial vortices* in superconducting films with the antidot lattices. However, the qualitative explanation of the magnetization anomalies observed at matching fields $H = H_m$ has not yet been found. Here the matching fields $H_m = m\phi_0/S$ are determined by the unit-cell area of the antidot lattice, S, and integer m. The interpretation of the experimental data[9–11] was hindered by the presence of the two different types of vortices (i) strongly pinned vortices at antidots and (ii) very weakly pinned interstitial vortices. These two types of vortices are formed due to the existence of shallow and deep minima in the pinning potential (Fig. 2) created at interstices and antidots, respectively, by the introduced antidot lattice[13] (Figs. 3 and 4). Interstitial vortices are much more mobile, which can be directly revealed in their enhanced flux-creep rate[10] and the shift of the onset of the Bardeen-Stephen flux-flow contribution to resistivity from $H = 0$ (reference nonperforated superconductor) to the particular field $H = H_m$ (perforated superconductor), beginning from which the interstitial vortices are formed.[14] These two types of vortices were already very briefly discussed by Fiory, Hebard, and Somekh[15] where it was suggested that cusplike magnetization $M(H)$ anomalies at matching fields H_m are typical for the formation of the FL lattices at antidots, whereas the peaklike $M(H)$ behavior at $H = H_m$ is characteristic for interstitial vortices. To avoid additional complications, related to the interstitial vortices, studied previously in Refs. 10, 11, and 14, we focus first in this paper on superconducting films with *relatively large antidots* which can successfully trap multiquanta vortices. We demonstrate that in this case puzzling sharp cusplike magnetization anomalies appearing at H_m are somewhat similar to the well-known $M(H)$ cusp at lower critical field H_{c1}, but for the onset of multiquanta vortices trapping by antidots: $2\phi_0$ at $H = H_1$, $3\phi_0$ at $H = H_2$, etc. Using the London limit expression for $M(H)$, we show that exactly at the matching fields H_m, magnetization is given by the relation $M(H_m) \propto -m\phi_0/\Lambda^2(T)$, where $\Lambda(T)$ is the temperature-

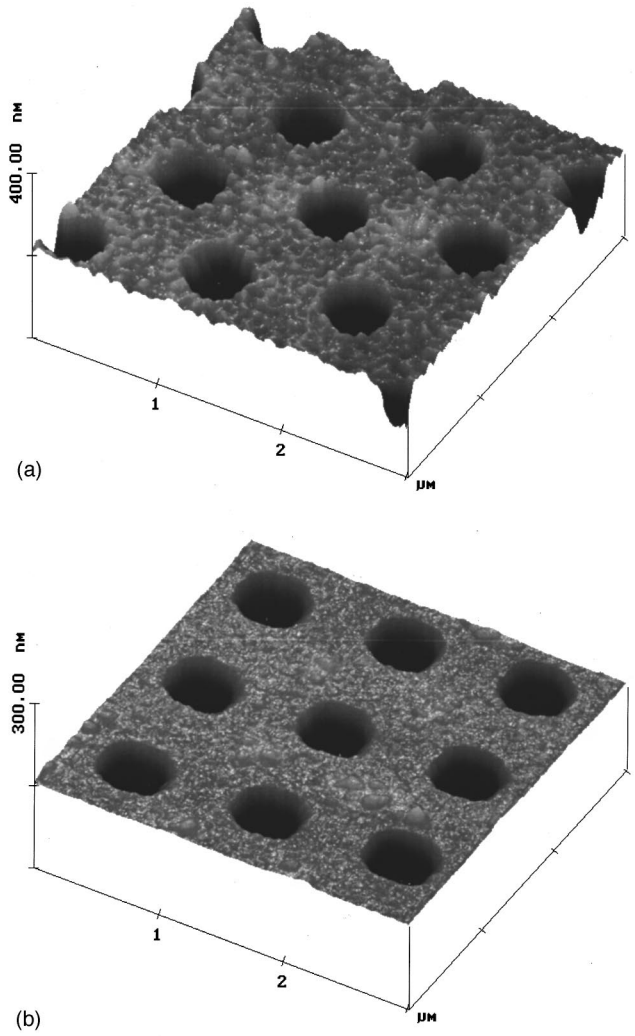

FIG. 1. An AFM picture of (a) a $[\mathrm{Pb}(100\ \text{Å})/\mathrm{Ge}(50\ \text{Å})]_2$ multilayer with a triangular lattice of submicron antidots (period $d=1\ \mu$m, radius $r\approx 0.22\ \mu$m) and (b) a WGe(600 Å) single film with a square lattice of antidots (period $d=1\ \mu$m, radius $r\approx 0.17\ \mu$m).

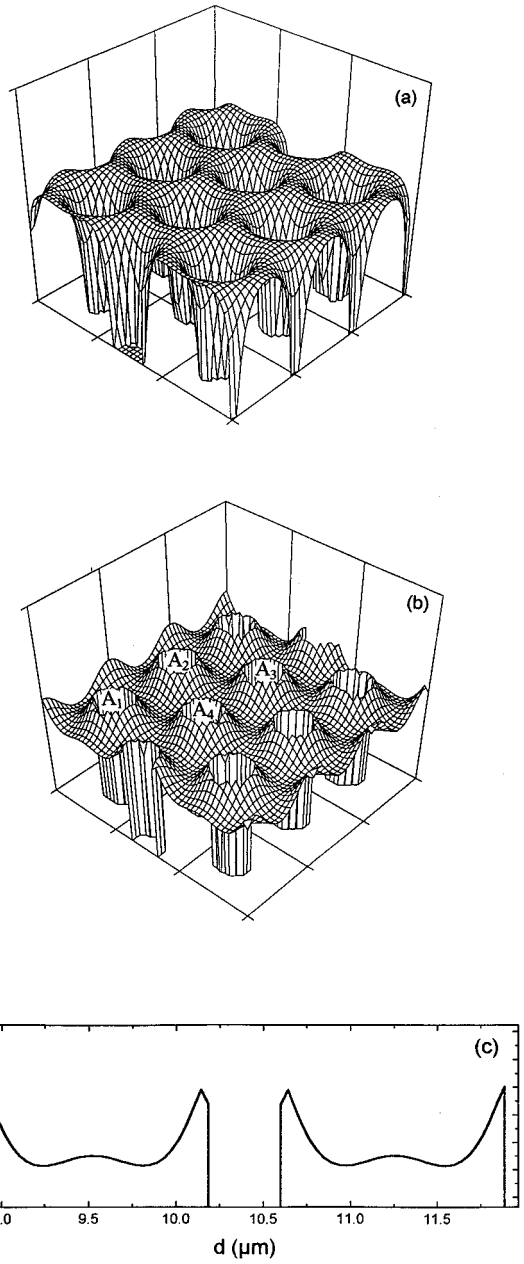

FIG. 2. Energy surface for one flux line in the cell of antidots, which was calculated with the following parameters: $\kappa=15$, $d=\lambda$, and $r=0.2\ \mu$m for (a) empty holes and (b) saturated holes (in Ginzburg-Landau units). In these calculations we have used the procedure described in Ref. 13. (c) A line cut connecting the points A_1A_3 of the energy surface shown in (b).

dependent penetration depth in thin films. Between the matching fields $H_m<H<H_{m+1}$, $M(H)$ follows the logarithmic behavior $M\propto-\ln(H-H_m)$ typical for the system of strongly inreracting FL. In other words, well known $M\propto-\ln H$ behavior of type-II superconductors in the London limit in the case of films with multiquanta vortex lattices stabilized by the antidot lattice should be rewritten as $M\propto-\ln(H-H_m)$. Therefore, the whole magnetization curve of superconducting films with an antidot lattice is now successfully described by the simple $M(H)$ expression, derived for interacting multiquanta vortices in the London limit. This consistent quantitative analysis of the magnetic behavior convincingly demonstrates the existence of multiple-ϕ_0 FL lattices in superconducting films with antidot lattices and opens new possibilities to control the width of the $M(H)$ hysteresis loop and critical current in nanostructured superconducting films. The crossover between the multiquanta and composite[10] vortex lattices is realized in fields $H>H_{n_s}$ when the antidots are saturated and vortices are forced to occupy interstices. The characteristic crossover field follows the temperature dependence expected from the saturation number $n_s=r/2\xi(T)$.

II. EXPERIMENTAL DETAILS

We have carried out the $M(H)$ measurements on high-quality nonperforated and perforated $[\mathrm{Pb}(100\ \text{Å})/\mathrm{Ge}(50\ \text{Å})]_n$ multilayers ($n=2$ bilayers) and amorphous $W_{1-x}Ge_x(600\ \text{Å})$ ($x\approx 0.33$) single films. Both were prepared in molecular-beam epitaxy apparatus using liquid-nitrogen cooled SiO_2 substrates. The WGe films were obtained by electron-beam

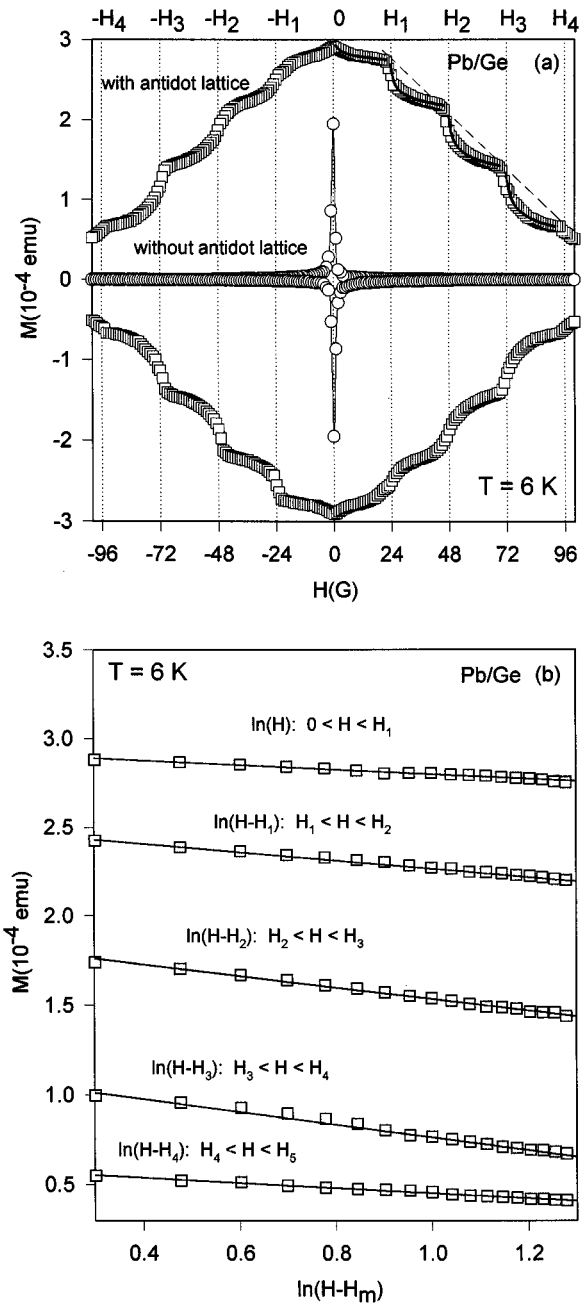

FIG. 3. (a) Magnetization loop $M(H)$ at $T=6$ K of a [Pb(100 Å)/Ge(50 Å)]$_2$ multilayer with and without the antidot lattice. The solid line is a fit with Eq. (4) (see text). The dashed line is demonstrating the validity of the linear behavior of $M(H_m)$ [Eq. (2)]. The loops were measured for $M>0$ and symmetrized for clarity for $M<0$. (b) The magnetization M versus $\ln(H-H_m)$ at $T=6$ K. The different slopes of the solid lines for the different periods are used to determine the effective flux $\tilde{\phi}_{0m}$ in Eq. (4).

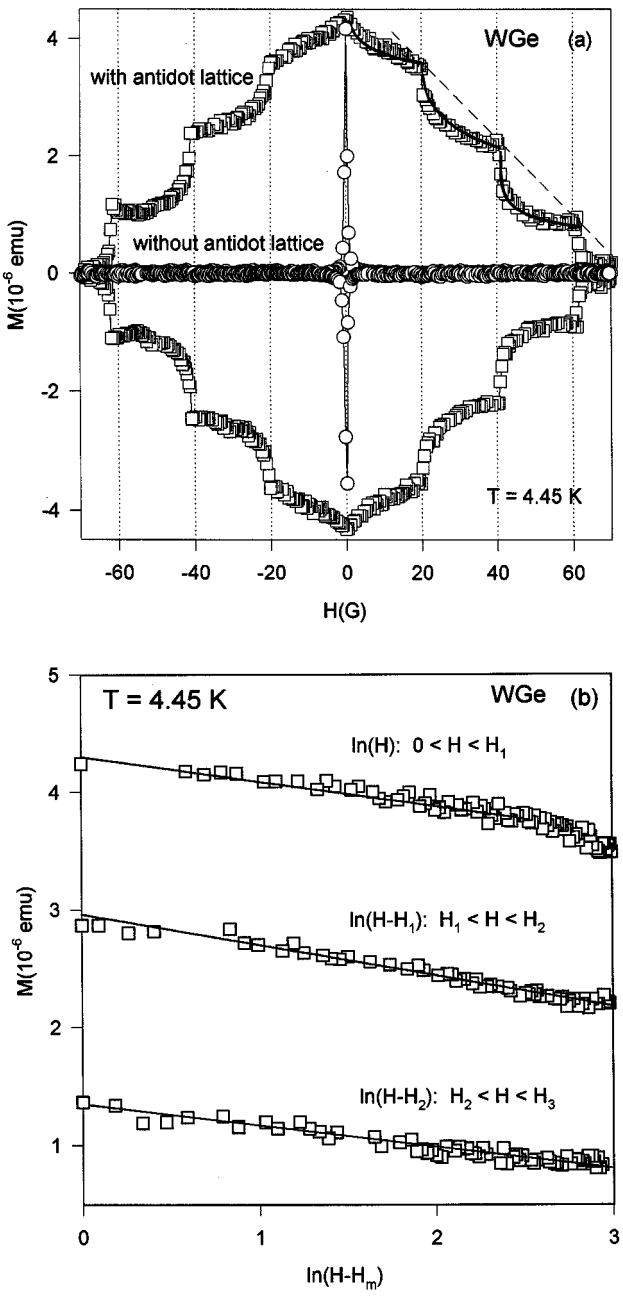

FIG. 4. (a) Magnetization loop $M(H)$ at $T=4.45$ K of a WGe(600 Å) single film with and without the antidot lattice. The solid line is a fit with Eq. (4) (see text). The dashed line is demonstrating the validity of the linear behavior of $M(H_m)$ [Eq. (2)]. The loops were measured for $M>0$ and symmetrized for clarity for $M<0$. (b) The magnetization M versus $\ln(H-H_m)$ at $T=4.45$ K. The different slopes of the solid lines for the different periods are used to determine the effective flux $\tilde{\phi}_{0m}$ in Eq. (4).

coevaporation of W and Ge. In the same films antidot lattices were fabricated by e-beam lithography (for details of the sample preparation see Ref. 16). Figure 1 shows a typical atomic force microscopy (AFM) picture of a Pb/Ge multilayer with a triangular [Fig. 1(a)] and a WGe single film with a square [Fig. 1(b)] ''antidot'' lattice. In Fig. 1(a) the distance d between the holes of radius $r=0.22$ μm is 1 μm and the surface between them is quite flat, the root-mean-square roughness σ is 4 nm on a (0.5 μm)^2 area. The antidots obtained in the WGe single films have radius of $r=0.17$ μm and σ of the surface between them is even less than in Pb/Ge: about 1 nm. The number of antidots per sample unit area is about 10^6/mm^2. The matching fields H_m for these perforated films, with a triangular antidot lattice, are $m\times 23.9$ G, while for a square antidot lattice $m\times 20.7$ G. The coherence length and penetration depth are $\xi(0)=120$ Å and $\lambda(0)=2600$ Å for the Pb/Ge multilayers while $\xi(0)=60$ Å and

$\lambda(0)=4900$ Å for the WGe single films. Magnetization measurements were performed in a commercial Quantum Design superconducting quantum interference device magnetometer with a scan length of 3 cm, corresponding to a field homogeneity better than 0.05%. Normally the cycle with decreasing field was used to measure $M(H)$ for $M>0$. It has also been carefully checked that the full hysteresis loop coincides with the loop obtained by taking the decreasing field branch of $M(H)$ and symmetrizing it for $M<0$ for increasing field.

III. MAGNETIZATION LOOPS OF SUPERCONDUCTING FILMS WITH AN ANTIDOT LATTICE

Typical magnetization loops $M(H,T_0)$ of superconducting films with square and triangular antidot lattices for temperatures T_0 close to T_c are shown in Figs. 3 and 4, with T_0 a fixed temperature. The $M(H,T_0)$ curves were also measured for reference Pb/Ge and WGe nonperforated films. The width ΔM of the $M(H,T_0)$ loops in perforated films is strongly increased due to the efficiency of antidots as artificial pinning centers. At the used temperatures not very far from T_c, the difference between the width of the hysteresis loops ΔM (Figs. 3 and 4) for as-grown and perforated films is so large (very high ''contrast''), that the $M(H,T_0)$ curves for the latter can be solely attributed to the contribution arising from the FL pinning by an antidot lattice.

Besides an overall enhancement of ΔM, distinct cusplike $M(H,T_0)$ anomalies are clearly seen exactly at the expected matching fields: $H_m=m\times 23.9$ G and $m\times 20.7$ G for triangular and square antidot lattices, respectively. Strictly speaking, there is always a shift in the position of the matching field H_m extracted from increasing ($H_m\uparrow$) and decreasing ($H_m\downarrow$) field measurements of $M(H)$. However, sufficiently close to T_c ($T_c-T\cong 1$ K), where the discussed sharp matching $M(H)$ anomalies are observed, the difference $\Delta H_m=(H_m\uparrow)-(H_m\downarrow)$ is very small. At lower temperatures matching $M(H)$ anomalies are smeared out and simultaneously the difference ΔH_m strongly increases. The radii of the used antidots in this work are sufficiently large, so that the nominal calculated saturation number[6] $n_s=r/2\xi(T)\approx 3.3$ for Pb/Ge multilayers at $T=6$ K ($T_c\approx 6.9$ K) and $n_s\approx 2$ for WGE single films at $T=4.45$ K ($T_c\sim 4.53$ K). In this case, we can assume that cusplike $M(H,T_c)$ anomalies are related to the formation of the multiquanta vortex lattices. One should keep in mind, that n_s calculated above is only a rough estimate of the saturation number since it was derived in the limit of FL's interacting with a single microhole.[6] Below, we shall be able to demonstrate, however, that the assumption of the existence of multiquanta vortex lattices is fully supported by a quantitative description of the whole magnetization curve.

IV. MULTIQUANTA VORTEX LATTICES

In this section we consider the situation when all vortices are trapped by the antidots and due to that there are no interstitial vortices. We begin with the estimate of the temperature-dependent penetration length $\Lambda=2\lambda^2/t$ (where λ is the penetration depth and t the total thickness of the film). The estimate of Λ shows that in our case $\Lambda(T=6\text{ K})\cong 5.8$ μm$\gg d=1$ μm. This Λ value can be even further increased due to the renormalization of the penetration depth in perforated films, where superconducting volume corrections have to be taken into account.[17] Since $\Lambda\gg d$, the approximation $B=$const (here B is to be averaged at least over several unit cells) can be used to find the magnetization M of the superconductor with the antidot lattice in the field range $H<H_1$ at temperatures quite close to T_c.

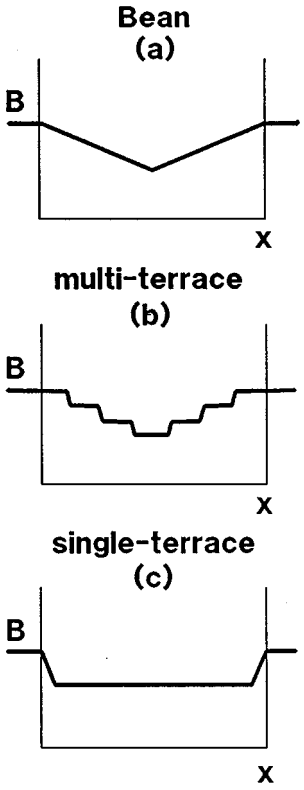

FIG. 5. The field penetration according to (a) the classical Bean model (Ref. 20), (b) the multiterrace critical state (Ref. 19), and (c) the single-terrace critical state.

There are at least two arguments in favor of the $B=$const approximation. The first one is the particular profile of the calculated field distribution in thin superconducting specimens.[18] For very large Λ the field inside the specimen is constant everywhere, except edges and the center. This field distribution provides constant field not in the whole sample but at least in a very large part of its area. The second argument in favor of the approximation $B(x)=$const can be based on the possibility of the existence of a single-terrace critical state in superconducting films with antidot lattices. Indeed, according to Cooley and Grishin,[19] the classical Bean model[20] [Fig. 5(a)] should be substantially modified for superconductors with a regular array of artificial pinning centers which favor a certain integer number of flux quanta pinned by each antidot. In this case, instead of a smooth sand-hill-like critical $B(x)$ profile [Fig. 5(a)], a multiterrace critical state with several well-defined plateaus, each having its own fixed induction $B(x)=$const, has been predicted [Fig. 5(b)].[19] The multiterrace critical state is, in a way, a quantized version of the classical Bean model. The field profile with well-defined terraces is a compromise between a tendency to trap the same number $m\phi_0$ of flux quanta by each antidot and a formation of a certain average Bean-like $B(x)$

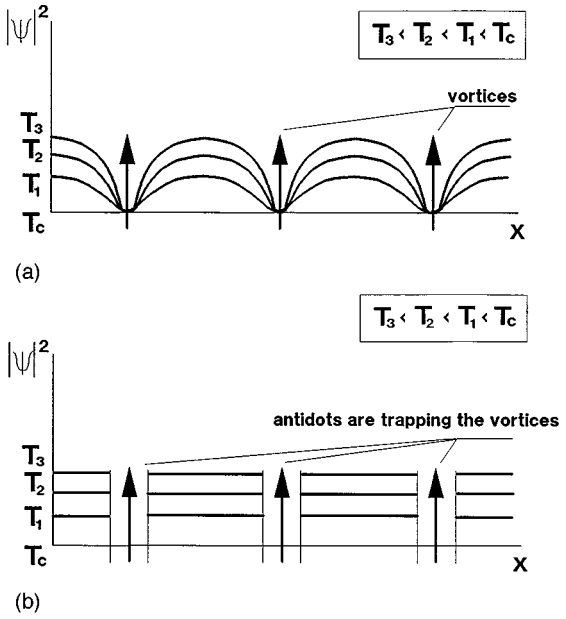

FIG. 6. The $|\psi|$ modulation in a homogeneous superconductor in the mixed state (a) and in a superconductor with an antidot lattice (b).

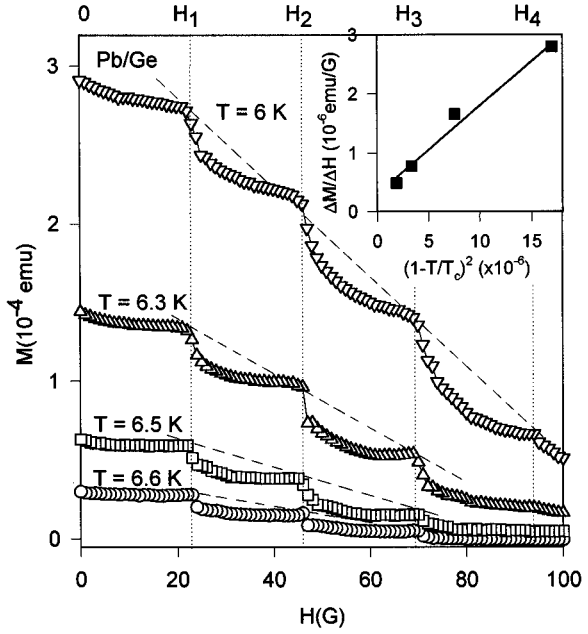

FIG. 7. The right upper parts of the magnetization loops $M(H)$ at different temperatures for the $[\mathrm{Pb}(100\ \text{Å})/\mathrm{Ge}(50\ \text{Å})]_2$ multilayer with an antidot lattice. The dashed lines, at different temperatures, clearly indicate the linear behavior of $M(H_m)$ as a function of the integer m. The inset presents the slopes $\Delta M/\Delta H$ of the dashed lines, as a function of $[1-(T/T_c)]^2$. According to Eq. (2) these slopes follow the temperature dependence of $1/\Lambda^2$. The solid line presents the linear fit.

slope. Close to T_c, $(T_c-T\cong 1\ \mathrm{K})$, the latter can be quite small and then an ultimate limit of the multiterrace critical state—a *single-terrace critical state* [Fig. 5(c)]—could be established. This state, especially exactly at matching fields, implies the flat field penetration profile $B(x)=\text{const}$ may be realized in the whole sample, except its surface layer.

The next important step towards the understanding of magnetization of the multiquanta vortices can be made by taking into account a possible expansion of the London limit $|\psi|=\text{constant}$ in superconducting films with antidot lattices. Indeed, in homogeneous superconductors in the vicinity of the upper critical field $H_{c2}(T)$ the superconducting order parameter $\psi=|\psi|e^{i\varphi}$ nucleates with a very strong $|\psi|$ modulation [Fig. 6(a)], in agreement with the classical Abrikosov model.[1] Due to this modulation the London limit can only be used in the range $H_{c1}\ll H\ll H_{c2}$, i.e., well below the $H_{c2}(T)$ line. Contrary to that, in a superconductor with an antidot lattice, by making antidots exactly at the expected positions for the penetration of vortices, we are ''helping'' the superconducting order parameter to nucleate in a different way [Fig. 6(b)]. In this case we are forcing $|\psi|$ to be nearly constant in the space between antidots, since due to boundary conditions at the superconductor-insulator interface[5] the surface $|\psi|=\text{const}$ can cross the cylinders, corresponding to the antidot boundaries, only at the angle 90°. Moreover, when FL's are guided to penetrate through the antidots, there is no need to create additional zeros of $\psi(r)$ (and therefore strong $|\psi|$ modulation) anywhere else. These arguments make it possible to foresee a broader range of validity of the London limit $|\psi|=\text{const}$ in films with an antidot lattice.

Taking into consideration the two important assumptions: $B=\text{const}$ and $|\psi|=\text{const}$, we can use now the textbook expression for magnetization[5] with a simple substitution $\xi(T)\rightarrow r$ for the core size:

$$M(H)=-\frac{\phi_0}{16\pi^2\Lambda^2}\ln\left(\frac{\beta a_\nu}{\sqrt{e}r}\right), \tag{1}$$

where a_ν is distance between ϕ_0 vortices, β is a numerical constant, for triangular vortex lattice in unperforated films $\beta=0.381$.[5]

First, let us consider a very interesting situation, which occurs *exactly at the matching fields* $H=H_m$, when we expect that the FL lattice consists of only one type of vortices, namely, of $m\phi_0$ vortices forming a regular array coinciding with the antidot lattice. In this case in Eq. (1) $m\phi_0$ should be used instead of ϕ_0 and $a_\nu=d$:

$$M(H_m)=-\frac{m\phi_0}{16\pi^2\Lambda^2}\ln\left(\frac{\beta d}{\sqrt{e}r}\right)\propto\frac{m\phi_0}{\Lambda^2}. \tag{2}$$

The difference $M(H_m)-M(H_{m-1})\propto-\phi_0/\Lambda^2$ is independent of m and is determined only by Λ. *All other parameters in Eq. (2) are known.* Therefore, at $H=H_m$ a linear behavior of $M(H_m)$ as a function of the integer m should be seen. This behavior is in a very good agreement with the observed $M(H_m)$ variation at different temperatures (see the dashed lines in Figs. 7 and 8). The slope of the dashed lines nicely follows the expected temperature variation of $1/\Lambda^2\propto(1-T/T_c)^2$ (inset of Figs. 7 and 8). The two-fluid model $1/\Lambda^2\propto[1-(T/T_c)^4]^2$ also gives a good fit, but the Ginzburg-Landau relation $\lambda(T)\propto 1/\sqrt{1-T/T_c}$ or $1/\lambda^2\propto 1-T/T_c$ provides a better linearity of the slope $\Delta M/\Delta H$ versus T (see inset of Figs. 7 and 8).

The cusps at $H=H_m$ then can be considered as analogs of the well-known $M(H)$ anomaly at H_{c1} but this time for the

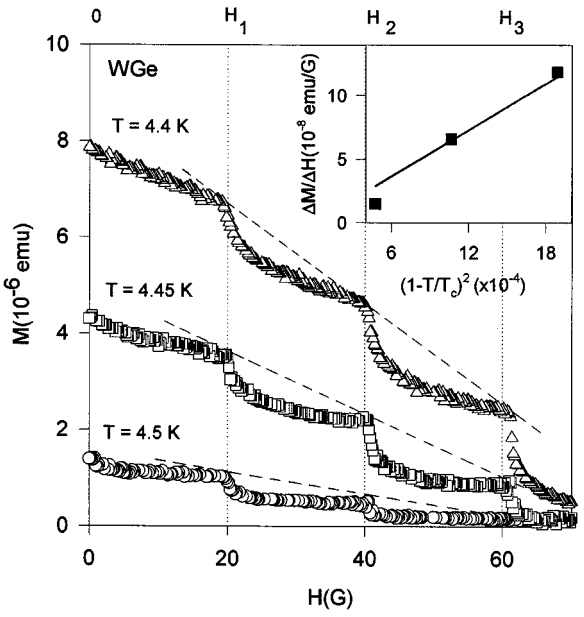

FIG. 8. The right upper parts of the magnetization loops $M(H)$ at different temperatures for a WGe(600 Å) single film with an antidot lattice. The dashed lines, at different temperatures, clearly indicate the linear behavior of $M(H_m)$ as a function of the integer m. The inset presents the slopes $\Delta M/\Delta H$ of the dashed lines, as a function of $[1-(T/T_c)]^2$. According to Eq. (2) these slopes follow the temperature dependence of $1/\Lambda^2$. The solid line presents the linear fit.

onset of penetration of $2\phi_0$, $3\phi_0$,..., $(m+1)\phi_0$ vortices at $H_1, H_2, \ldots, H_m$, respectively. Indeed, the expected lower critical fields $H_{c1}(m\phi_0)$ are

$$H_{c1}(m\phi_0) = \frac{m\phi_0}{4\pi\Lambda^2} \ln\frac{\Lambda}{r}. \tag{3}$$

The estimate based on Eq. (3) gives very low fields $H_{c1}(m\phi_0) \sim 10^{-2}$ Oe$\ll H_m$, which implies that the difference between $H-H_m-H_{c1}[(m+1)\phi_0]$ and $H-H_m$ can be neglected and therefore one should see the logarithmic behavior $M(H) \propto -\ln(H-H_m)$ (valid for $H \gg H_{c1}$ in the London limit) in magnetic fields $H_m < H < H_{m+1}$, i.e., between the matching fields. Such behavior is fully supported by our experimental data (Figs. 3 and 4). This behavior is a result of inserting the relation $a_\nu \cong [\phi_0/(H-H_m)]^{1/2}$ into Eq. (1), which is a good approximation in fields $H_m < H < H_{m+1}$ for a $(m+1)\phi_0$ vortex-vortex distance in a superconductor with an antidot lattice. In this interval the vortex-vortex interaction terms U_{ij} in the Gibbs potential are represented by different contributions arising from the presence of two types of vortices: $m\phi_0$ and $(m+1)\phi_0$. These terms will contain instead of the usual $\phi_0 \times \phi_0$ product,[5] other products: $m\phi_0 \times m\phi_0$, $m\phi_0 \times (m+1)\phi_0$, and $(m+1)\phi_0 \times (m+1)\phi_0$. Due to that, in the interval between the matching fields, H_m and H_{m+1}, magnetization of the superconducting films with an antidot lattice should follow the logarithmic dependence:

$$M(H_m < H < H_{m+1}) \cong -\frac{\tilde{\phi}_{0m}}{16\pi^2\Lambda^2} \ln\left[\frac{\beta_{\rm eff}}{\sqrt{e}r}\left(\frac{\phi_0}{H-H_m}\right)^{1/2}\right]. \tag{4}$$

Here $\tilde{\phi}_{0m}$ is an effective flux and $\beta_{\rm eff}$ an effective parameter appearing due to the summation of different terms in the vortex-vortex interactions U_{ij} over vortex positions i and j on the antidot lattice. For H not far from H_m we may approximate $\tilde{\phi}_{0m}$ as $\sqrt{m(m+1)}\phi_0$.

Plotting M versus $\ln(H-H_m)$ (Fig. 7), from a logarithmic behavior of the magnetization (Fig. 3), we determined the slopes of the M versus $\ln(H-H_m)$ lines which give us the effective flux $\tilde{\phi}_{0m}$. For a triangular antidot lattice stabilizing the multiquanta vortices we have $\tilde{\phi}_{01}/\phi_0=1$; $\tilde{\phi}_{02}/\phi_0=1.79$; $\tilde{\phi}_{03}/\phi_0=2.45$; $\tilde{\phi}_{04}/\phi_0=2.72$, for $H_0<H<H_1$, $H_1<H<H_2$, $H_2<H<H_3$, respectively. The decrease of the slope for $H>H_4$ [Fig. 3(b)] will be discussed in Sec. V. The numbers 1.79, 2.45, and 2.72 have to be compared with 1.41, 2.45, and 3.46 estimated from $[\sqrt{m(m+1)}\phi_0]/\phi_0$. Therefore, besides a logarithmic dependence itself, we see also a very reasonable variation of an effective parameter $\tilde{\phi}_{0m}$ in different field intervals $(H_m<H<H_{m+1})$ with m not exceeding the saturation number n_s. At higher temperatures the simple argument that $\tilde{\phi}_{0m}$ should scale as $\sqrt{m(m+1)}\phi_0$ fails, since $\lambda(T)$ is spread over many periods and U_{ij} terms, corresponding to $m\phi_0 \times (m+1)\phi_0$ and $(m+1)\phi_0 \times (m+1)\phi_0$, should be optimized numerically.[21] These terms can also explain a small increase of magnetization when H is approaching the matching fields from below (see Fig. 3).

We also would like to note that the stabilization of the FL by the antidot lattice has resulted in a remarkable collective $M(H)$ behavior, typical for the presence of a $m\phi_0$-FL lattice at $H=H_m$ $(m<n_s)$ and a mixture of $m\phi_0$ and $(m+1)\phi_0$ vortices between the matching fields $H_m<H\leq_{m+1}$. Due to the introduction of the well-defined pinning potential, we were able to obtain in a multiple-connected superconductor with an antidot lattice the *logarithmic irreversible magnetization behavior* which is normally observed as a *reversible magnetization of the Abrikosov FL lattice* in homogeneous superconductors in fields $H \gg H_{c1}$. We think that the irreversibility of the perforated film is mainly caused by its multiple connectivity. The superconducting currents flowing around antidots are quite similar to a supercurrent in a ring. As it was already emphasized by Shoenberg quite some time ago (see, for example, Ref. 22 and references therein), a ring, as a multiply connected body, demonstrates a strong irreversible magnetization response.

The successful interpretation of all specific features of the magnetization loops for films with an antidot lattice [Figs. 3(a) and 4(a)] gives a strong support of the assumption of the existence of the multiquanta vortex lattices. Recent magnetic decoration experiments[23] have convincingly and directly confirmed the stabilization of the multiquanta vortices by the relatively large antidots. In these experiments the use of the ''blind holes'' has made it possible to decorate the multiquanta vortices at antidots and thus to count the number of the flux quanta trapped by each antidot. Direct experimental observation of multiquanta vortex lattices with no vortices pinned at the interstices confirms our conclusions based on the analysis of the magnetization data.

V. FROM MULTIQUANTA TO COMPOSITE VORTEX LATTICES

The saturation number $n_s = r/2\xi(T)$ can be varied by changing both the size of the antidots and temperature, since

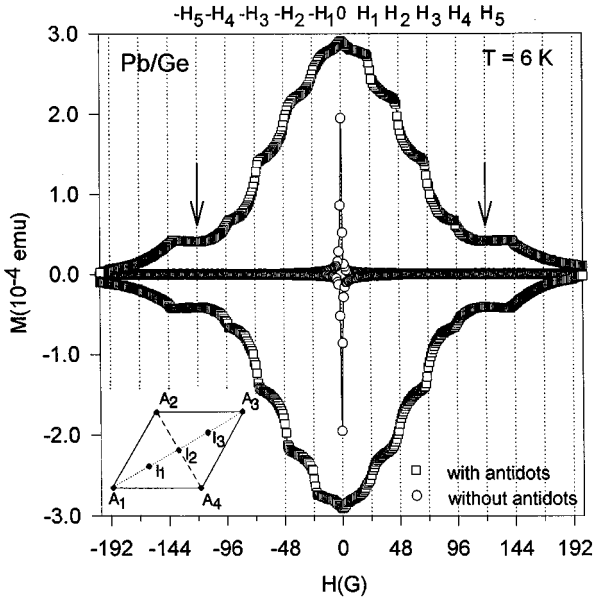

FIG. 9. Magnetization loop $M(H)$ at $T=6$ K of a [Pb(100 Å)/Ge(50 Å)]$_2$ multilayer with and without the antidot lattice measured in a broader field range. The inset shows the parallelogram $A_1A_2A_3A_4$ formed by the antidots. Interstitial flux lines will be pinned at the positions I_1 and I_3.

the coherence length $\xi(T)$ increases substantially when $T\rightarrow T_c$. Therefore, even for a fixed antidot radius r, different types of vortex lattices can be realized by tuning temperature into a proper interval and thus changing n_s. We begin with the magnetization data taken at the lowest used temperature $T=6$ K, (Fig. 9), when the width of the hysteresis loop $M(H)$ has allowed us to observe a finite loop width in a broader field range up to 200 G. The $M(H)$ curve for the films with an antidot lattice demonstrates, as we have already seen before four successive cusplike anomalies at $H=H_1,\ldots,H_4$ corresponding to the formation of the vortex lattices carrying $\phi_0,\ldots,4\phi_0$ flux quanta.

Therefore, it is reasonable to assume that in this case the saturation number is at least four, which is close to the value expected from the calculated ratio $r/2\xi(T)\simeq 3.3$ at $T=6$ K. However, in higher fields, at $H=H_5$, the next matching anomaly does not show up. This mysterious disappearance of the matching cusp can be interpreted as an indication of the onset of pinning of vortices by interstices. Indeed, the position ''I_2'' in the center of the parallelogram $A_1A_2A_3A_4$ (see inset of Fig. 9) formed by the antidots is a saddle point in the pinning potential produced by the antidots A_1-A_3 [see Fig. 2(c)]. As a result, interstitial flux lines will be pinned at the two equivalent positions I_1 and I_3 corresponding to the two minima of the pinning potential. The number of the flux lines required to fill in the antidot lattice all positions of the type I_1 and I_3 is twice as large as the number of the antidots with all interstitial positions filled by FL's, the formation of the $5\phi_0$ vortices at antidots seems to occur only at $H=H_6$ (Fig. 9). This explains the ''mystery'' of the missing $M(H)$ cusp at $H=H_5$ (Fig. 9) and gives a strong evidence that at $H=H_4$ antidots are indeed saturated, i.e., at $T=6$ K, $n_s=4$.

The formation of the interstitial vortices can also be detected from the decrease of the slopes of the logarithmic plots M versus $\ln(H-H_3)$ and M versus $\ln(H-H_4)$ [see Fig. 3(b)]. As expected, the latter is noticeably smaller than the former. This can be interpreted as a consequence of the presence of the single-quantum flux lines at interstices for $H>H_4$, which leads to the substitution of the expected effective flux $\tilde{\phi}_{0m}(H_4<H<H_5)\sim\sqrt{4\times 5}\phi_0$, if the $5\phi_0$ vortices were formed at antidots, by a quite different value $\tilde{\phi}_{0m}(H_4<H<H_5)\sim\sqrt{1\times 4}\phi_0$, since, instead of adding the fifth ϕ_0 flux into the antidot, vortices go to interstitial positions at $H>H_4$. The calculated ratio $\sqrt{3\times 4}/\sqrt{1\times 4}=\sqrt{3}$ of the slopes of the M versus $\ln(H-H_3)$ and M versus $\ln(H-H_4)$ curves is in agreement with the measured ratio ≈ 2 [see Fig. 3(b)]. It is difficult to expect a better correspondence between the two ratios, since Eq. (4) most probably will not remain exactly the same if the coexistence of the vortices at antidots and interstices is taken into consideration. In any case, a substantial reduction of the M versus $\ln(H-H_4)$ slope at $H=H_4$ with respect to the slope at $H=H_3$ [see Fig. 3(b)] is a clear evidence of the formation of the vortices with a much smaller flux per vortex than the flux expected for the lattice consisting of the $5\phi_0$ vortices.

The assigned saturation number $n_s=4$ at $T=6$ K can also be checked by investigating the variation of the sequence of matching anomalies in magnetization curves at different temperatures. Since the saturation number n_s simply defines the cusplike matching anomaly at $H=H_{n_S}$ followed by the missing cusp at $H=H_{n_S+1}$, the decrease in $n_s=r/2\xi(T)$ caused by the increase of $\xi(T)$ at higher temperatures, should also lead to a shift of the missing $M(H)$ cusp at H_{n_S+1}. Figure 10(a) ($T=6.5$ K, $n_s=3$) and Fig. 10(b) ($T=6.7$ K, $n_s=2$) convincingly demonstrate that this is indeed the case: at $T=6.5$ K there is no matching peak at H_4 and then at $T=6.7$ K a very sharp cusp at H_2 precedes a missing cusp at H_3. The variation of n_s with temperature is summarized in Fig. 11 where temperature dependence of n_s correlates well with the temperature dependence of $1/\xi(T)\propto(1-T/T_c)^{1/2}$ (dashed line). It should also be added, that besides our observations based mostly on magnetization data, the interplay between pinning by antidots and interstices has also been seen in magnetic decoration experiments.[23]

The pinning potential at antidots and at interstices is very different (Fig. 2) and it is also very sensitive to the temperature variation. As a result, as $T\rightarrow T_c$, the minima of the pinning potential at interstices become so shallow that they cannot pin any longer the interstitial vortices,[11] which will then form an interstitial flux fluid. Therefore by changing temperature, one can induce at interstices the crossover from the flux solid to the flux fluid.

Summarizing this section, we would like to emphasize the unique possibilities to stabilize flux phases in superconducting films by making regular arrays of pinning centers (in our case, antidots). These phases are

(i) *Multiquanta vortex lattices*. They can be realized if the antidots are sufficiently large and field does not exceed the value H_{n_S} defined by the saturation number n_s.

(ii) *Composite flux lattices*. These flux lattices are observed when the normalized radii of the antidots $r/[2\xi(T)]$ are sufficiently small and H exceeds the limiting field H_{n_S}. Also the pinning potential at interstices should not be very shallow to provide a weaker, but still sufficient pinning to

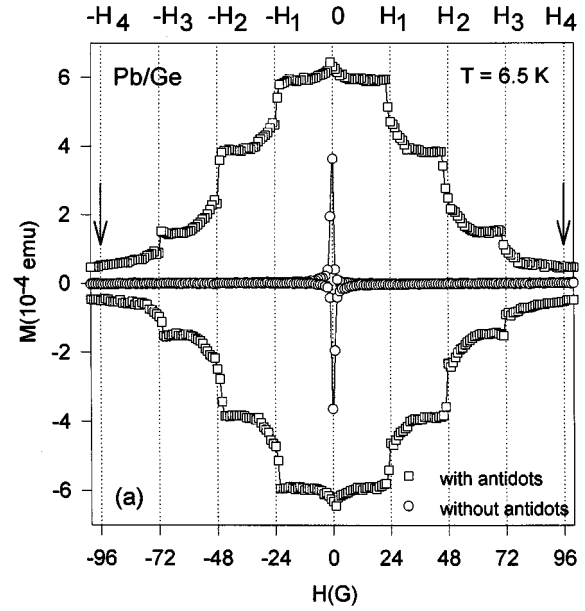

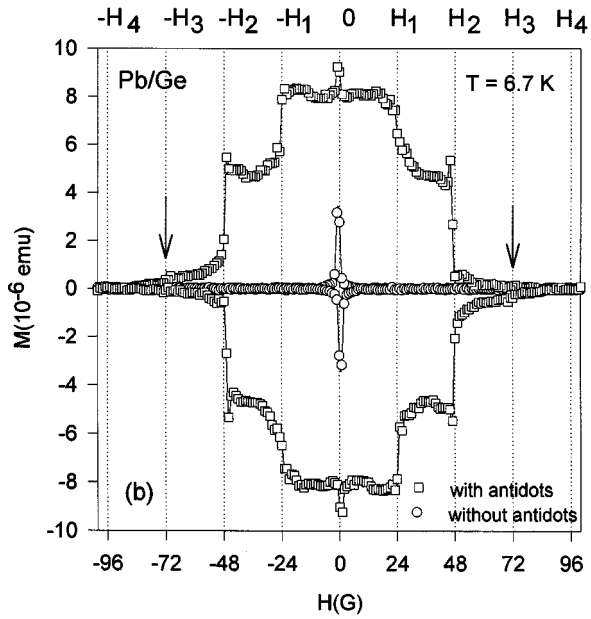

FIG. 10. Magnetization loop $M(H)$ of a $[\mathrm{Pb}(100\ \text{Å})/\mathrm{Ge}(50\ \text{Å})]_2$ multilayer with and without the antidot lattice (a) at $T=6.5$ K and (b) $T=6.7$ K. The arrows indicate the missing $M(H)$ cusp.

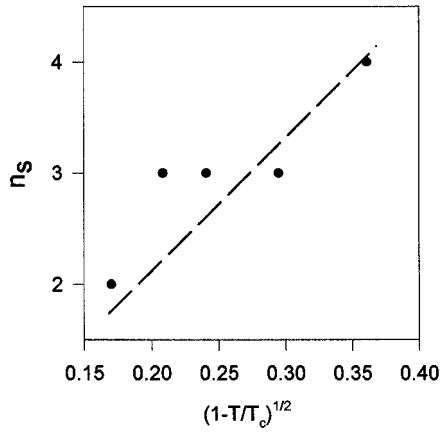

FIG. 11. The variation of the saturation value n_s with temperature. The temperature dependence of n_s correlates with the temperature dependence of $1/\xi(T)\propto(1-T/T_c)^{1/2}$ (dashed line).

form a softer interstitial flux solid. The composite flux lattices are characterized by the coexistence of the two—weakly and strongly pinned—interpenetrating flux lattices at interstices (ϕ_0 vortices) and antidots ($m\phi_0$ vortices), respectively.[11,14]

(iii) *Multiquanta vortex lattice coexisting with the interstitial fluid of ϕ_0 vortices*. This flux phase is formed when $T\rightarrow T_c$ and the interstitial pinning potential becomes very shallow and thus cannot prevent the melting of the caged interstitial pinning ϕ_0 vortices. The melting transition as a function of magnetic field is then observed exactly at $H=H_{n_S}$ [see, for example transition at $H=H_2$, $T=6.7$ K in Fig. 10(b) where for $H>H_2$ there is still a finite width of the hysteresis loop or a very abrupt first-order phase transition at $H=H_1$ and $T=6.8$ K in Ref. 10]. In other words, the homogeneous $m\phi_0$-vortex solid with $m=n_s$ produces in this case only the $B=$const background while the melting of the interstitial ϕ_0-vortex phase causes the very sharp magnetization drop at $H=H_{n_S}$. The interstitial vortex fluid reversibly responds to the field variation and this results in a zero width of the hysteresis loop in fields $H>H_{n_S}$.

The flux phases listed above can exist at temperatures not too far from T_c, since at lower temperatures the tendency to form a conventional Bean profile [Fig. 5(a)] starts to dominate and matching anomalies are suppressed, for example for Pb/Ge we barely see any $M(H)$ matching anomalies below 5 K.

VI. CONCLUSION

In conclusion, the superconducting film with a lattice of relatively large antidots seems to demonstrate the single-terrace critical state which appears due to the multiple connectivity of the film and the stabilization of the $m\phi_0$-flux lattices. The separation of the areas where flux penetrates from those where the superconducting order parameter nucleates provides a kind of a ''peaceful coexistence'' of FL's pinned by antidots with the superconducting condensate in the space between them. Fabricating an antidot lattice to let flux go through, we are thus helping the order parameter between the antidots to sustain much higher currents and magnetic fields. The presence of the antidot lattice also broadens the validity of the London limit. Using the two essential assumptions: $B=$const (single-terrace critical state, especially at matching fields $H=H_m$) and $|\psi|=$const, we have reached close to T_c a convincing quantitative description of the magnetization loops, including linear behavior of $M(H)$ at matching fields $M(H_m)\propto -m\phi_0/\Lambda^2$ and logarithmic behavior elsewhere: $M(H_m<H<H_{m+1})\propto -\ln(H-H_m)$. By varying the saturation number $n_s=r/2\xi(T)$

through the use of different $\xi(T)$, we have demonstrated that the missing matching cusp at $H=H_{n_s+1}$, signaling the onset of the formation of the interstitial vortices at $H>H_{n_s}$ is systematically shifted to lower matching fields as $T\rightarrow T_c$. The existence of several flux phases—multiquanta vortex lattice, composite flux lattice, and interstitial ϕ_0-vortex fluid coexisting with the $m\phi_0$-vortex lattices at antidots—is briefly discussed.

ACKNOWLEDGMENTS

This work was supported by the National Fund for Scientific Research (NFWO) and Concerted Action (GOA) Programs. We would like to acknowledge useful discussions with C. Van Haesendonck. M.B. was supported by the IUAP programs and V. V. Metlushko was supported by the Research Council of the University of Leuven.

[1] A. A. Abrikosov, Sov. Phys. JETP **5**, 1174 (1957).

[2] U. Esmann and H. Trauble, Phys. Lett. **24A**, 526 (1967).

[3] J. Schelten, H. Ullmaier, and W. Schmatz, Phys. Status Solidi B **48**, 619 (1971).

[4] H. F. Hess, C. A. Murray, and J. V. Waszczak, Phys. Rev. Lett. **69**, 2138 (1992).

[5] P. G. de Gennes, *Superconductivity of Metals and Alloys* (Addison-Wesley, New York, 1966).

[6] G. S. Mkrtchyan and V. V. Shmidt, Sov. Phys. JETP **34**, 195 (1972).

[7] A. I. Buzdin, Phys. Rev. B **47**, 11 416 (1993).

[8] A. F. Hebard, A. T. Fiory, and S. Somekh, IEEE Trans. Magn. **1**, 589 (1977).

[9] V. V. Moshchalkov, L. Gielen, M. Baert, V. V. Metlushko, G. Neuttiens, C. Strunk, V. Bruyndoncx, X. Qiu, M. Dhallé, K. Temst, C. D. Potter, R. Jonckheere, L. Stockman, M. Van Bael, C. Van Haesendonck, and Y. Bruynseraede, Phys. Scr. **T55**, 168 (1994).

[10] M. Baert, V. V. Metlushko, R. Jonckheere, V. V. Moshchalkov, and Y. Bruynseraede, Phys. Rev. Lett. **74**, 3269 (1995).

[11] M. Baert, V. V. Metlushko, R. Jonckheere, V. V. Moshchalkov, and Y. Bruynseraede, Europhys. Lett. **29(2)**, 157 (1995).

[12] H. Fang, R. Zeller, and P. J. Stiles, Appl. Phys. Lett. **55**, 1433 (1989); K. Ensslin and P. M. Petroff, Phys. Rev. B **41**, 12 307 (1990).

[13] I. B. Khalfin and B. Ya. Shapiro, Physica C **207**, 359 (1993).

[14] E. Rosseel, M. Van Bael, M. Baert, R. Jonckheere, V. V. Moshchalkov, and Y. Bruynseraede, Phys. Rev. B **53**, R2983 (1996).

[15] A. T. Fiory, A. F. Hebard, and S. Somekh, Appl. Phys. Lett. **32(1)**, 73 (1978).

[16] Y. Bruynseraede, K. Temst, E. Osquiguil, C. Van Haesendonck, A. Gilabert, and I. K. Schuller, Phys. Scr. T **42**, 37 (1992).

[17] A. Wahl, V. Hardy, J. Provost, Ch. Simon, and A. Buzdin, Physica C **250**, 163 (1995).

[18] E. S. Bakhanova and V. M. Genkin, in *Applied Superconductivity*, edited by H. C. Freyhardt (DGM Informationgesellschaft, Göttingen, 1993).

[19] L. D. Cooley and A. M. Grishin, Phys. Rev. Lett. **74**, 2788 (1995).

[20] C. P. Bean, Phys. Rev. Lett. **8**, 250 (1962).

[21] X. Qiu *et al.* (unpublished).

[22] D. Shoenberg, *Superconductivity* (Cambridge University Press, Cambridge, MA, 1965).

[23] B. Pannetier *et al.* (unpublished); A. Bezryadin and B. Pannetier, J. Low Temp. Phys. **102**, 73 (1996).